

RESEARCH

Open Access



# A 'golden' alternative for prevention of cisplatin nephrotoxicity in bladder cancer

Yoray Sharon<sup>1</sup>, Menachem Motiei<sup>2</sup>, Chen Tzror-Azankot<sup>2</sup>, Tamar Sadan<sup>2</sup>, Rachela Popovtzer<sup>2\*</sup> and Eli Rosenbaum<sup>1\*</sup>

\*Correspondence:  
rachela.popovtzer@biu.ac.il;  
eliros@clalit.org.il

<sup>1</sup> Institute of Oncology, Davidoff Center, Rabin Medical Center, Petah Tikvah, Israel

<sup>2</sup> Faculty of Engineering and the Institute of Nanotechnology & Advanced Materials, Bar-Ilan University, 5290002 Ramat Gan, Israel

## Abstract

Cisplatin (CP) is the first-line standard of care for bladder cancer. However, a significant percentage of advanced bladder cancer patients are ineligible to receive standard CP treatment, due to the drug's toxicity, and in particular its nephrotoxicity. These patients currently face suboptimal therapeutic options with lower efficacy. To overcome this limitation, here we designed CP-conjugated gold nanoparticles (GNPs) with specific properties that prevent renal toxicity, and concurrently preserve the therapeutic efficacy of CP. Safety and efficacy of the particles were studied in bladder tumor-bearing mice, using clinically-relevant fractionated or non-fractionated dosing regimens. A non-fractionated high dose of CP-GNP showed long-term intratumoral accumulation, blocked tumor growth, and nullified the lethal effect of CP. Treatment with fractionated lower doses of CP-GNP was also superior to an equivalent treatment with free CP, demonstrating both anti-tumor efficacy and prolonged mouse survival. Moreover, as opposed to free drug, CP-conjugated GNPs did not cause fibrosis or necrosis in kidney. These results indicate that conjugating CP to GNPs can serve as an effective, combined anti-cancer and renoprotective approach, and thus has potential to widen the range of patients eligible for CP-based therapy.

**Keywords:** Cisplatin, Gold nanoparticles, Drug delivery, Bladder cancer, Nephrotoxicity

## Background

Bladder cancer is prevalent worldwide and can manifest in aggressive and invasive tumors with high mortality. A large proportion (40–50%) of advanced bladder cancer patients have impaired renal function, due to multiple factors, including age, medical comorbidities, and in particular ureteral obstruction by tumor infiltration (Dash et al. 2006; Ichioka et al. 2015). Cisplatin (CP), a prominent platinum chemotherapy (Vita et al. 2001), is the preferred first-line standard of care for bladder cancer (Lavoie et al. 2021). However, nephrotoxicity is one of CP's most common and significant side effects (Hartmann et al. 1999). CP has enhanced transporter-mediated uptake into renal tubular cells (Goldstein and Mayor 1983), resulting in intracellular accumulation and tubular cell damage and death (Shirali and Perazella 2014; Perazella 2012; Perazella and Moeckel 2010). Renal impaired patients currently



face suboptimal therapeutic options, such as fractionated treatment with lower CP doses (Jiang et al. 2021), or other less nephrotoxic chemotherapies, such as carboplatin-based therapy, usually with gemcitabine, and a minority with non-platinum-based therapy, such as gemcitabine and paclitaxel (Wheate et al. 2010). These drugs are inferior alternatives to CP, due to their lower response rates and poorer overall survival outcomes (Sideris et al. 2016). Hence, there is need for a new approach to CP-based treatment, which can deliver the drug to the bladder tumor, while sparing renal function.

Nanoparticles are one of the most effective platforms for delivering drugs to solid tumors (Stylianopoulos 2013; Gao et al. 2021; Kumar et al. 2013). Nanoparticles passively target tumors by preferentially extravasating through the permeable tumor vasculature and are retained there due to reduced lymphatic drainage (Gao et al. 2021), a phenomenon known as the enhanced permeability and retention (EPR) effect. In particular, gold nanoparticles (GNPs) are excellent drug carriers, due to their biocompatibility and non-immunogenicity, and as they enable a wide range of surface modifications and simple tuning of physical characteristics (Hsu et al. 2020). Thus, GNPs can be surface-modified with CP and easily tuned to a size that can, on one hand, effectively target tumors, while on the other hand prevent glomerular filtration and subsequent entrance into the tubular system (Huang et al. 2021). We have previously shown that GNPs conjugated to CP effectively target head and neck tumor xenografts in mice, and serve for combined chemotherapy delivery and radiosensitizing, as well as tumor imaging agents (Davidi et al. 2018). Taking together the unique characteristics of GNPs, we hypothesized that CP-GNP conjugation may have anti-tumor efficacy, and concomitantly prevent kidney toxicity, in bladder cancer.

Therefore, in the present study, we assessed the safety and efficacy of CP conjugated to GNPs as compared to free CP, at different dosing regimens, in MB49 bladder tumor-bearing mice. We found that non-fractionated (acute) high dose, or fractionated lower doses, of CP-GNP demonstrated anti-tumor efficacy, rescued from substantial CP-induced mortality, and had significantly lower renal toxicity as compared to free CP.

## Results

### Synthesis and characterization of CP-GNPs

Gold nanoparticles sized 20 nm were synthesized and coated with polyethylene glycol and then with CP. We have previously shown that this size is ideal for tumor accumulation (Dreifuss et al. 2015), and we hypothesized that it could also prevent reaching of tubules, as  $\geq 20$  nm nanoparticles cannot pass through the glomerular filtration barrier (Huang et al. 2021). Characterization of the particles was conducted using transmission electron microscopy (TEM), UV-Vis spectroscopy, and zeta potential measurements. TEM showed uniform, spherical GNPs, with average size of  $\sim 20$  nm in diameter (Fig. 1A). Hydrodynamic size of the CP-GNPs was a mean of  $33 \pm 2.6$  nm as measured by dynamic light scattering (DLS) (Fig. 1B). Successful coating of the nanoparticles was confirmed by zeta potential measurements (Fig. 1C) and by UV-Vis plasmon resonance (Fig. 1D).

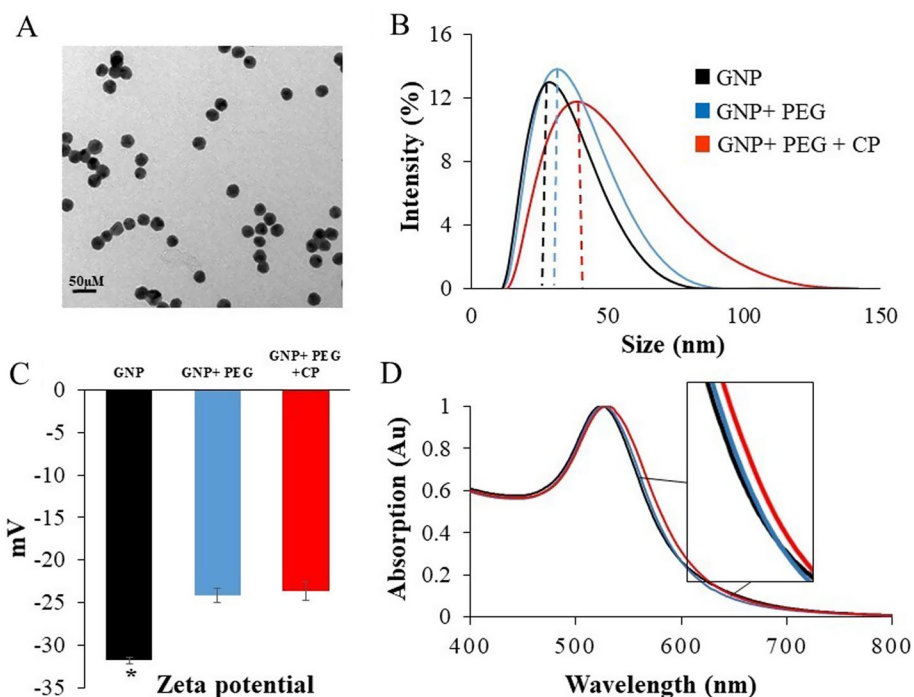


**Fig. 1** Characterization of CP-GNPs. **A.** Transmission electron microscopy image of ~20 nm spherical GNPs. **B.** Hydrodynamic size measurements of the GNPs over the synthesis stages—bare GNPs, PEG-coated GNPs, and the final CP-GNPs. **C.** Zeta potential measurements of the GNP synthesis stages. **D.** UV-Vis spectroscopy of the GNP synthesis stages (key in panel **B**)

**Cytotoxic effect of CP-GNPs on bladder cancer cells**

CP-GNP cytotoxicity was evaluated as compared to that of equivalent amounts of free CP or free GNPs, in the MB49 bladder carcinoma cell line. Cells were incubated (37 °C) for 48 h with either CP-GNPs (7.3 μM CP; 78.4 μg Au), free CP (7.3 μM), or free GNPs (78.4 μg), and then assessed for survival. As compared to untreated controls, treatment with free CP or CP-GNPs resulted in more than 40% cell mortality at 48 h post treatment (Fig. 2). Free GNPs did not affect cell viability. These results indicate that CP-GNPs

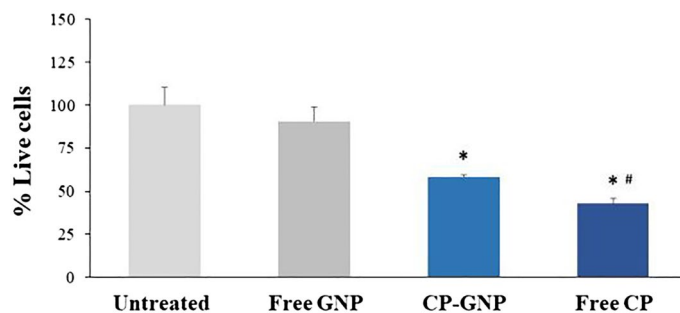


**Fig. 2** Cytotoxic effect of CP-GNPs on MB49 bladder cancer cell line. Percentage of live cells either untreated or after incubation of 48 h with free GNPs, CP-GNPs, or free CP. Free CP and CP-GNP treatments significantly lowered cell survival. \**p* < 0.05 for free CP or CP-GNP-treated cells vs. untreated and free GNP-treated cells; #*p* < 0.05 free CP vs. CP-GNP; Student’s t-test

have a cytotoxic effect on MB49 bladder cancer cells, and that this is due to CP coating, and not to the GNPs themselves.

### CP-GNPs dose- and time-dependently accumulate in bladder tumor

First, the ability of different doses of IP-injected CP-GNPs to accumulate within a bladder tumor was investigated. MB49 tumor-bearing mice were treated with an IP injection of either 13 mg/kg, 20 mg/kg or 50 mg/kg GNP-CP, and after 14 days, the intra-tumoral Pt levels were quantified by inductively coupled plasma optical emission spectrometry (ICP-OES). The higher doses of 20 mg/kg and 50 mg/kg CP-GNP showed significantly higher intra-tumoral accumulation as compared to 13 mg/kg CP-GNP ( $p < 0.05$ ; Fig. 3A). To elucidate tumor uptake, we assessed the biodistribution of the different doses within major organs (Additional file 1: Figure S1). The majority of CP-GNPs was found to accumulate in reticuloendothelial system organs, which suggests that the lower dose resulted in a relatively low tumor accumulation that was not detected after 14 days.

Next, the tumor accumulation of a single IP injection of 20 mg/kg CP-GNP was compared to that of an equivalent dose of free CP, known to cause nephrotoxicity and mortality in mice. Four days after treatment of MB49 tumor-bearing mice, ICP-OES analysis showed significantly higher levels of CP-GNP than free CP within tumors ( $p < 0.05$ ; Fig. 3B). The higher intra-tumoral accumulation of GNPs is likely due to its different pharmacokinetics and the EPR effect as shown in literature (Gao et al. 2021) and also supported by analysis of clearance organs in the treated mice (Additional file 1: Figure S2A). In most major organs, Pt levels in free CP treated mice were significantly lower than those of CP-GNP treated mice. Total amount of Pt in organs and blood of free CP treated mice was 7.5-fold lower than that in CP-GNP treated mice (total of 0.02 vs. 0.15 mg Pt/gr tissue, respectively), indicating more rapid clearance of free drug (Additional file 1: Figure S2B). Interestingly, free CP treated mice had 23.6% of total Pt in kidney, while CP-GNP treated mice had only 2.6% of total Pt in the kidney (Additional file 1: Figure S2B).

Longitudinal comparison of CP-GNP levels within the MB49 tumor after the single 20 mg/kg injection showed significantly higher levels 4 days after treatment as compared

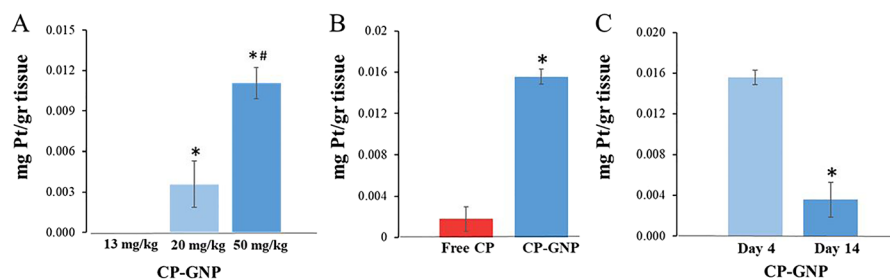


**Fig. 3** MB49 bladder tumor accumulation of CP-GNPs. Intra-tumoral accumulation of increasing doses of CP-GNP was measured in MB49-tumor bearing mice using ICP-OES. **A** 20 mg/kg and 50 mg/kg CP-GNP showed significantly higher intra-tumoral accumulation than the lower 13 mg/kg dose on day 14 after administration. \* $p < 0.05$  for 20 mg/kg and 50 mg/kg vs. 13 mg/kg; # $p < 0.05$  for 50 mg/kg vs. 20 mg/kg; Student's t-test. **B** Intra-tumoral accumulation of 20 mg/kg CP-GNP was significantly higher than that of 20 mg/kg free CP, on day 4 after administration. \* $p < 0.05$ , Student's t-test. **C** Intra-tumoral accumulation of 20 mg/kg CP-GNP 4 day post-administration was significantly higher than that on day 14 post-administration. \* $p < 0.05$ , Student's t-test

to 14 days after treatment, indicating clearance of CP-GNP from the tumor over time ( $p < 0.05$ ; Fig. 3C). This result is supported by analysis of major organs (Additional file 1: Figure S3). Nonetheless, the clear presence of CP-GNPs in the tumor even 14 days after a single treatment indicates that they may have a long-term effect on the tumor.

#### **CP-GNPs have anti-tumor efficacy and nullify the lethal effect of high dose CP**

In the clinic, bladder cancer patients with normal kidney function receive a full (non-fractionated) high dose of CP. As we found above that a single high dose of CP-GNPs showed long-term accumulation in bladder tumors, we next investigated whether this treatment has therapeutic efficacy and safety.

To this end, MB49 tumor-bearing mice were treated with a single IP injection of either 20 mg/kg free CP or CP-GNPs, and monitored over 2 weeks for the effect on tumor volume, weight, and survival. Untreated MB49 tumor-bearing mice served as controls. Free CP treatment was found to impair tumor growth ( $p < 0.05$  vs. untreated), yet it nonetheless led to significant weight reduction, as well as rapid and significant ~75% mortality 4 days after treatment, and to complete mortality up to day 9 ( $p < 0.005$ ,  $\chi^2$  test) (Fig. 4A–C). These results are in accordance with the literature, showing mortality of mice in a matter of days after such a single high-dose CP injection (Perše and Veceric-Haler 2018). In contrast, an equivalent dose of CP-GNPs significantly inhibited tumor growth as compared to controls, up to 14 days after injection ( $p < 0.05$ ; Student's t-test; Fig. 4A). Weight in CP-GNP-treated mice was not affected as compared to controls up to day 14, and notably, the mice in this group survived throughout the study (Fig. 4B, C).

Taken together, these results indicate that a single high dose of CP-GNPs has a potent and long-term effect on tumor growth, and concomitantly nullifies the lethal effect of CP.

Histological analysis of kidneys at 4 days post treatment revealed a moderate-to-severe tubulo-necrosis, and protein accumulation (nephropathy) with some glomerular changes only in free CP-treated mice, and not in CP-GNP treated and control groups (Fig. 5A). Necrosis score was significantly higher for free CP as compared to untreated and CP-GNP treated mice ( $p < 0.05$ ; Fig. 5B).

#### **Fractionated CP-GNP treatment is superior to fractionated free CP treatment**

To minimize clinical nephrotoxicity, bladder cancer patients with borderline impaired renal function can receive an alternative compromised regimen of fractionated CP treatment (Jiang et al. 2021). Hence, we next assessed the safety and efficacy of fractionated CP-GNPs as compared to free CP. Over the course of 20 days, MB49 tumor-bearing mice received fractionated doses of either free CP or CP-GNPs (as detailed in Methods), during which tumor volume, survival and weight were monitored, followed by nephrotoxicity analysis. Untreated MB49 tumor-bearing mice served as controls.

Fractionated free CP inhibited tumor growth ( $p < 0.05$  vs. untreated), yet it nonetheless induced significant weight reduction, as well as significant 61% mortality by day 11 ( $p < 0.005$ ,  $\chi^2$  test) (Fig. 6A–C). It is notable that the relative increase in average weight in this group from day 11 was due to the significant mortality rate that occurred from this timepoint, and not to reduction in CP's toxic effect.

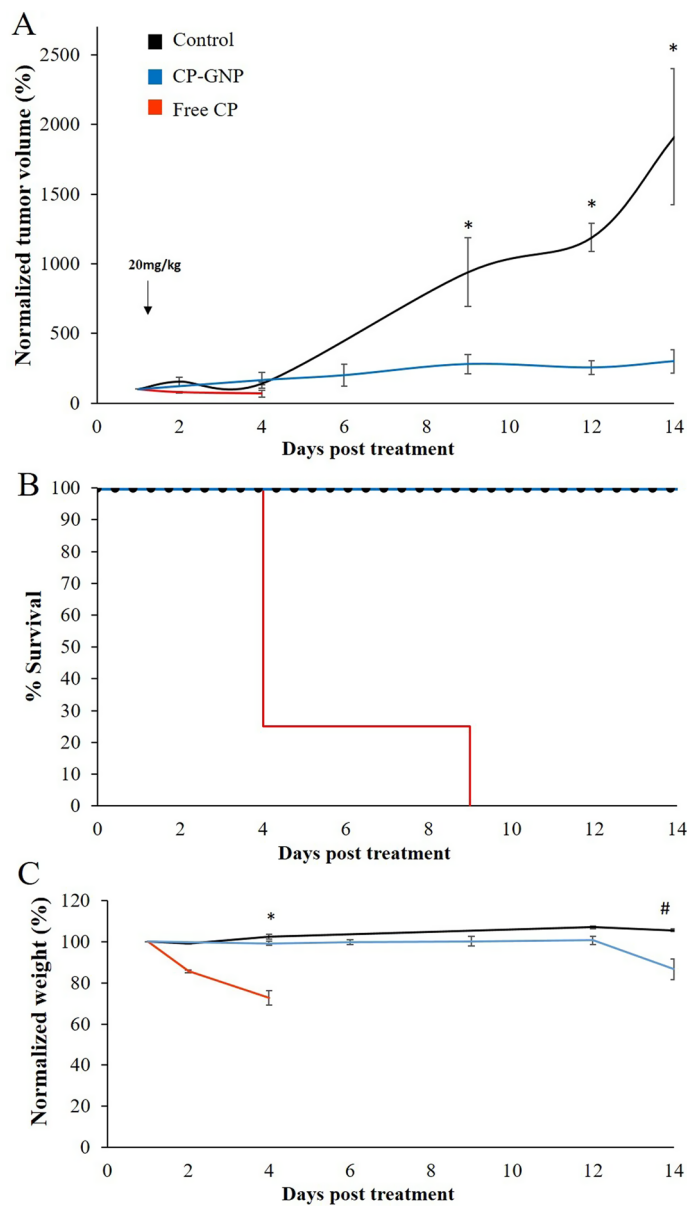


**Fig. 4** Effect of single high-dose CP or CP-GNP injection on MB49 tumor-bearing mice. **A** Tumor growth was inhibited in free CP-treated and CP-GNP-treated mice as compared to untreated mice. Tumor growth normalized to initial volume. \* $p < 0.05$  vs. untreated, Student's t test. **B** Kaplan–Meier survival curve. Early mortality occurred in CP-treated mice as compared to prolonged survival of CP-GNP treated mice. **C** Weight level in CP-treated mice was significantly reduced as compared to untreated; weight in CP-GNP-treated mice remained steady except for a decrease on day 14 ( $p < 0.05$  for \*free CP-treated and #CP-GNP treated vs. untreated; Student's t-test. Weight and tumor growth results presented as mean  $\pm$  SEM

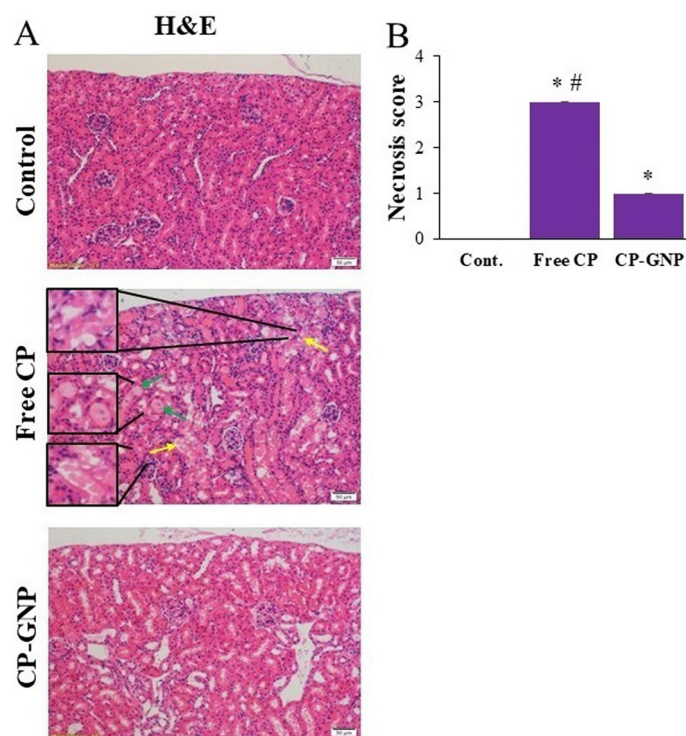


**Fig. 5** Histological analysis of kidneys in treated mice. **A**) Kidneys were excised at 4 day post-treatment and stained with H&E, revealing moderate-to-severe tubulo-necrosis, and nephropathy manifested as protein accumulation with some glomerular changes in free CP-treated mice, in contrast to CP-GNP treated and control groups. **B**) Necrosis scores, free CP-treated mice vs. untreated (\* $p < 0.05$ ), free CP-treated vs. CP-GNP treated mice ( $\#p < 0.05$ ), CP-GNP-treated vs. untreated (\* $p < 0.05$ ; Student's t-test)

Fractionated GNP-CP treatment led to significant inhibition of tumor growth as compared to untreated mice ( $p < 0.05$ , Student's t-test). Moreover, mice in this group had steady weight levels, along with prolonged survival up to the end of the study (Fig. 6A–C).

Histological analysis of kidneys was conducted by classical H&E staining and additional Masson trichome analysis of the fibrosis state, as fibrosis is known to be a late onset manifestation of tissue damage. Histological analysis of kidneys of free CP-treated mice revealed lesions characterized by local fibrosis and tubular necrosis with cellular debris in the lumina (Fig. 7). In contrast, no pathological changes were found in kidneys of CP-GNP treated mice, similar to untreated controls. Both necrosis and fibrosis scores were significantly higher for free CP as compared to untreated and CP-GNP treated mice ( $p < 0.05$ ) (Fig. 7).

Taken together, our results show anti-tumor efficacy of fractionated CP-GNP, with no observed toxicity, in particular in the kidney.

## Discussion

In the present study, we investigated the effect of CP conjugation to GNPs on the drug's anti-tumor efficacy, general toxicity and nephrotoxicity, in a mouse model of bladder cancer. In vitro, CP-GNPs effectively reduced cell viability. In vivo, CP-GNP

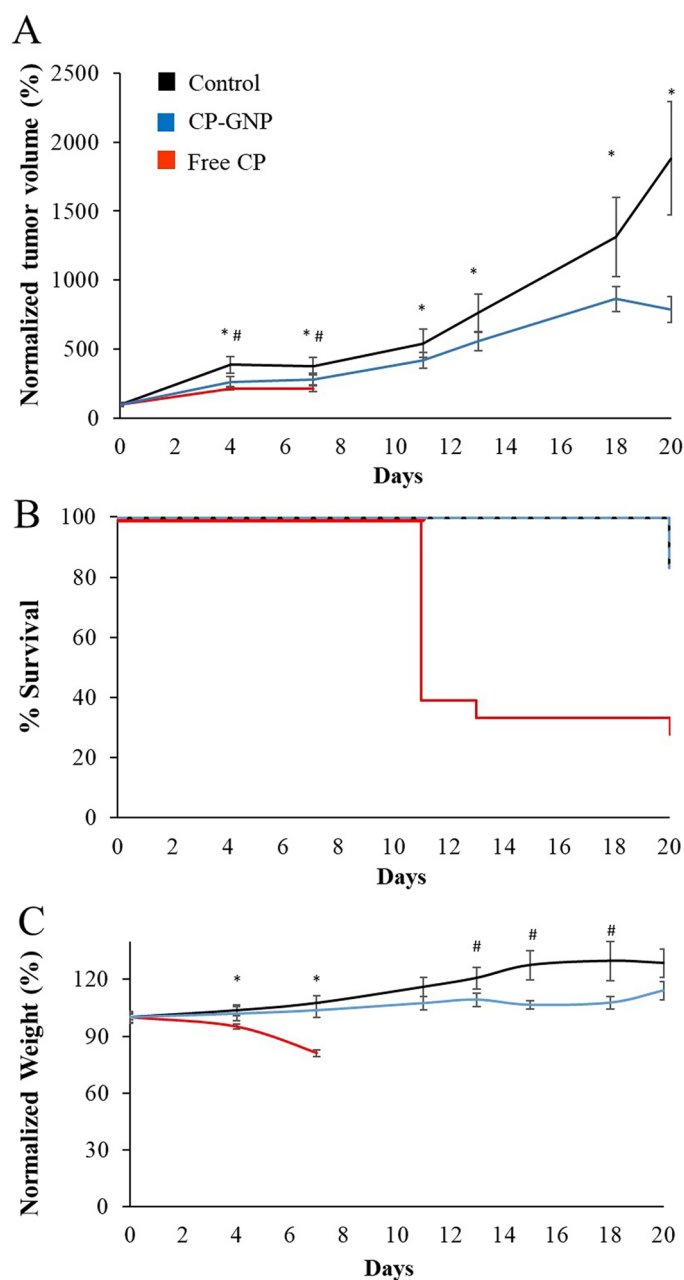


**Fig. 6** Effect of fractionated CP-GNP on tumor growth and general toxicity. **A** Tumor growth in free CP-treated, CP-GNP-treated and untreated mice. Growth normalized to initial volume.  $p < 0.05$  for \*free CP-treated and #CP-GNP-treated vs. untreated; Student's t-test. **B** Kaplan–Meier survival curve showing prolonged survival of CP-GNP-treated mice as opposed to CP-treated mice. **C** Weight levels in treated and untreated mice. \* $p < 0.05$  free CP treated vs. untreated (days 4–20); # $p < 0.05$  CP-GNP treated vs. untreated from days 13–20 (Student's t test). Weight normalized to initial weight. Results presented as mean  $\pm$  SEM

demonstrated time- and dose-dependent accumulation in bladder tumor, which was higher than that of free drug. Two different dosing regimens with CP-GNPs, i.e., an acute high dose or repeated low dose fractionated treatments, both showed safety, as opposed to the lethality of equivalent treatments with free CP. In addition to nullifying



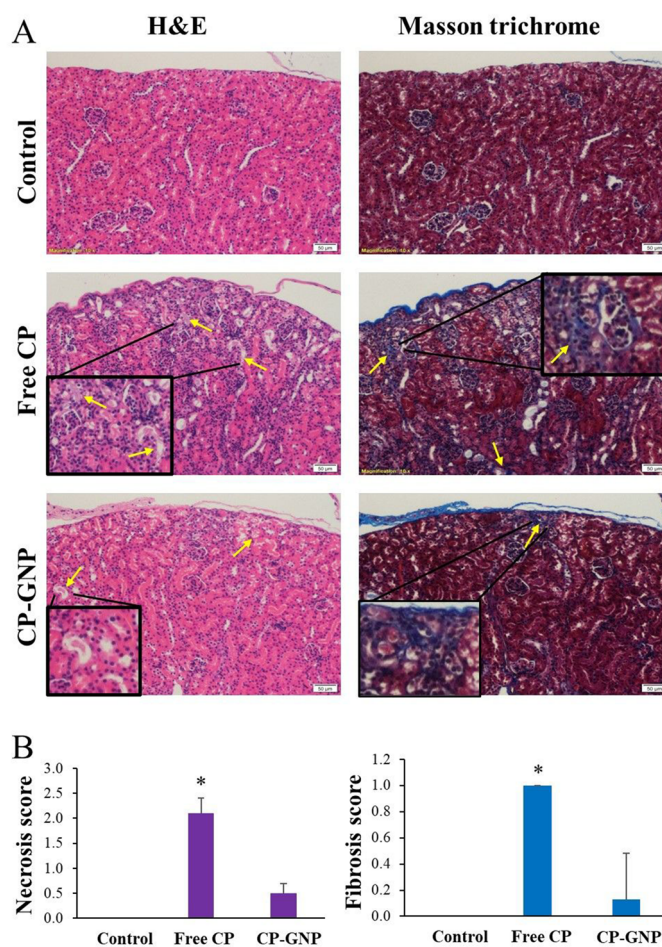


**Fig. 7** Effect of free CP or CP-GNP on kidney. **A** Histological analysis of kidneys in free CP-treated mice showed lesions characterized by a necrosis process in tubules cellular debris in the lumina (H&E staining), and fibrosis (Masson's trichrome stain). Yellow arrows indicate sample pathological changes in kidney sections. Magnification 10x. Scale bar = 50  $\mu$ m. Black square demarcates zoom-in of sample area in each section. **B** Necrosis and fibrosis scores for free CP-treated, CP-GNP-treated and untreated control groups. Results presented as mean  $\pm$  SEM. *Cont.* Control

CP-induced toxicity and nephrotoxicity, CP-GNPs showed long-term inhibition of tumor growth, in either dosing regimen.

Although CP is one of the most potent chemotherapies and a gold-standard treatment for bladder cancer, its nephrotoxicity is a limiting side effect that renders close to 50% of bladder cancer patients ineligible to receive the drug (Dash et al. 2006; Ichioka et al. 2015). Luminal transport of CP into tubular cells is a crucial element in the drug's nephrotoxicity. Extensive research has found that cisplatin entry into a cell is facilitated by a number of cellular transporters, including the primary transporters human copper transport protein 1 (Ctr1) and the organic cation transporter 2 (OCT2) which are expressed on renal tubular cells (Manohar and Leung 2018). Once cisplatin enters the tubular cell, it has been noted to exert many effects which culminate in apoptosis/necrosis of the cell. The commonly known damaged target is nuclear DNA, but multiple cellular targets have been identified over the past four decades, including

cytoplasmic organelle dysfunction, apoptotic pathways (both caspase-dependent and death receptor-mediated), oxidative stress with formation of reactive oxygen species, and inflammation (mediated via tumor necrosis factor and other chemokines (Manohar and Leung 2018). Therefore, it is of high importance to develop new technologies that prevent cisplatin from reaching the tubules and its uptake by its transporters. GNPs are an ideal technology for this purpose due to their biocompatibility, and ease of tuning and surface modification (Hsu et al. 2020).

Here, CP-GNP showed general safety in mice (i.e., no weight loss or mortality), as well as significantly less necrotic lesions (for both acute and repeated treatments) and less fibrosis (for repeated treatment) in the kidney, as compared to free CP. Moreover, the significantly lower percentage of total Pt in kidney for CP-GNP as compared to free CP treatment indicates that for free CP, extensive clearance likely occurs via the kidney, while for CP-GNPs there is low kidney clearance, as they likely bypass glomerular filtration. This is supported by the fact that nanoparticles larger than the glomerular filtration barrier size cutoff (~8–10 nm) do not pass through this barrier and cannot enter the tubule system (Huang et al. 2021), but are likely to return to the circulation for clearance by the liver and final elimination by feces (Zhang et al. 2016; Bourquin et al. 2018). Thus, it is likely that the 20 nm-sized CP-GNPs do not enter the tubule system, sparing them from CP-induced toxicity. This will be confirmed in future studies.

We have previously shown that IV administered 20 nm GNPs have no effect on well-being, hematology, and kidney or liver functions (Popovtzer et al. 2016), nor on food intake, weight, or neurological/coordination parameters (Hazkani et al. 2017) in tumor-bearing mice, which further supports the safety of GNP for treatment of tumors. Future studies will verify safety in additional organs and determine the exact mechanism underlying the general safety and prevention of renal toxicity by conjugation of CP to GNPs. It is notable that the safety of GNPs has been established in several clinical studies, showing that various types of GNPs (TNF-alpha conjugated GNPs for advanced solid tumors; GNP shell-silica core particles for prostate cancer; and siRNA conjugated GNPs for recurrent glioblastoma) were well-tolerated in patients, with no significant side effects (Libutti et al. 2010; Rastinehad et al. 2019; Stern et al. xxxx). This supports the further potential of CP-GNPs for clinical translation.

We further show high intra-tumoral accumulation of a single dose of CP-GNP, which remained in the tumor up to 14 days. This indicates that conjugation of CP to GNPs can improve accumulation of the drug at its tumor target, which likely contributes to its long-term inhibitive effect on tumor growth. These results also suggest that future CP-GNP-based treatments may enable longer intervals between treatments, which can have a positive impact on patient well-being.

Other nanoparticles delivering CP for cancer therapy have been shown, mostly polymeric and liposomal particles (Pourmadadi et al. 2022; Duan et al. 2016), in which the drug is encapsulated within the particle. CP-encapsulated liposomes have progressed to clinical trials, yet have failed to demonstrate efficacy, in part due to low drug loading because of the poor water solubility and low lipophilicity of cisplatin (Duan et al. 2016), a challenge that can be circumvented using CP-GNPs. Previous studies have shown

cytotoxicity of CP conjugated to GNPs against cervical cancer (HeLa), gastric cancer (AGS) and glioblastoma (C6) cell lines in vitro (González-López et al. 2020). Other studies (Comenge et al. 2012), including ours (Davidi et al. 2018), have shown efficacy of CP conjugated to GNPs in vivo, and support current findings. In this study, to derive clinically-relevant insights, we chose to investigate dose and time-dependent tumor accumulation, as well as safety and anti-tumor efficacy of fractionated and non-fractionated dosing regimens of CP conjugated to GNP. It is notable that CP-GNPs have potential to be combined with other clinical treatments in cancer patients, including radiotherapy, and with computed tomography for image-guided therapy (Davidi et al. 2018).

## Conclusions

The current study is the first, to the best of our knowledge, to show that conjugating CP to GNPs is both safe and effective for treatment of bladder cancer. Conjugating CP to GNPs is a simple and straightforward approach, with potential to break the trade-off between CP's safety and efficacy, and to treat a wider range of patients- including those currently considered CP-ineligible—with higher drug doses while reducing overall toxicity.

## Materials and methods

### Synthesis and characterization of CP-GNPs

Synthesis of 20 nm spherical GNPs was carried out as previously described by Enustun and Turkevich (36). Briefly,  $\text{HAuCl}_4$  solution (414  $\mu\text{L}$  of 50% w/v ( was added to double distilled water) 200 ml(, followed by heating in an oil bath until boiling. Then, 4.04 ml of 10% solution of sodium citrate tribasic dihydrate (Sigma-Aldrich, Rehovot, Israel) was added, followed by 10 min stirring. After cooling to room temperature GNPs were coated with a layer of polyethylene glycol (9.47 mg SH-PEGCOOH; MW  $\approx$  1 kDa; Sigma-Aldrich). The mixture was stirred for 24 h at room temperature. Glucosamine conjugation was performed by adding 52.5  $\mu\text{L}$  12 mg/mL D-(1)-glucosamine hydrochloride (Sigma-Aldrich) followed by excess EDC (1-ethyl- 3-(3-(dimethylamino)propyl) carbodiimide HCl, Thermo Scientific) and NHS (N-hydroxysulfosuccinimide sodium salt, ChemImpex International). 2 mg of  $\text{Cl}_2\text{-Pt-(NH}_3)_2$  (Sigma-Aldrich) (1 mg/mL) was added to the mixture, and stirred overnight at room temperature. GNPs were then centrifuged to a final Au concentration of 30 mg  $\text{mL}^{-1}$  as measured by atomic absorption spectroscopy (Davidi et al. 2018).

Size, shape and uniformity of the GNPs were measured using transmission electron microscopy (TEM) (JEM-1400, JEOL). Samples were prepared by drop-casting 5  $\mu\text{L}$  of the GNP solution onto standard carbon-coated film on a cooper grid. Samples were left to dry in a vacuum desiccator. The GNPs were further characterized using ultraviolet-visible spectroscopy (UV-1650 PC; Shimadzu Corporation, Kyoto Japan), dynamic light scattering (DLS) and zeta-potential (ZetaSizer 3000HS; Malvern Instruments, Malvern, UK).

To confirm and quantify cisplatin conjugation to GNPs, the particles were washed (72 h dialysis) to eliminate any remains of unconjugated cisplatin, then Au and Pt were quantified by ICP-OES. This quantification served for the estimation that an Au concentration of 30 mg/mL contained 1.13 mg/mL cisplatin ( $\sim$ 2000 molecules of cisplatin

upon each GNP). To confirm conjugation stability CP-GNP were resuspended in saline for 24 h (in room temperature), dialyzed, and Au and Pt were then re-quantified by ICP-OES. Similar amounts of Au and Pt to those in the initial quantification were found.

#### **In vitro cell survival analysis**

MB49 mouse bladder cancer cell line (Merck, SCC148) was cultured in Dulbecco's modified Eagle's medium (DMEM; Biological Industries, Beth Haemek, Israel) supplemented with 10% heat-inactivated fetal bovine serum (FBS) (Biological Industries, Beth Haemek, Israel (BI)) and maintained in a 37 °C and 5% CO<sub>2</sub> incubator. This widely-used murine bladder cancer cell line shares several pivotal tumor characteristics with human bladder cancer, such as cell surface markers, sensitivity to apoptosis, and immunological profile (Liu et al. 2019). To assess cell survival, MB49 cells (10<sup>4</sup>) were seeded in 14 mm dishes and grown in 1 mL DMEM with 5% fetal calf serum, 0.5% penicillin and 0.5% glutamine. Cells were incubated at 37 °C with either CP-GNP (7.3 μM CP, 78.4 μg Au), CP (7.3 μM), free GNP (78.4 μg Au), or left untreated (*n* = 3 samples per group). After 48 h, medium was removed and cells were washed twice with PBS. To quantify live cells, the whole area of each seeded well was captured using a Leica DFC295 microscope camera (Wetzlar, Germany) at × 40 magnification. Adherent live cells in each well were then quantified by cell counter. In each group the percentage of live cells was calculated with respect to control cells (considered as 100%).

#### **Animal model and in vivo experiments**

The animal study was conducted in compliance with protocols approved by the Animal Care and Use Committees of Bar Ilan University, Ramat Gan, Israel, and performed in accordance with the National Institutes of Health guidelines and regulations.

For tumor induction, MB49 cells (100 μl; 10<sup>6</sup>) were injected subcutaneously into the back flank area of C57BL6 male mice aged 8 weeks (*n* = 7/group for the different treatments, detailed below). Treatments were administered intraperitoneally (IP) (Perše and Veceric-Haler 2018) once tumors reached a diameter of 5–8 mm (day 0).

#### **ICP-OES analysis**

To determine tumor accumulation of CP-GNP, tumor-bearing mice were treated IP with free CP or CP-GNPs (13 mg/kg, 20 mg/kg or 50 mg/kg CP, 30 mg/ml gold). The tumor was excised (on day 4 or 14) and melted in 1 mL aqua-regia acid (a mixture of nitric acid and hydrochloric acid in a volume ratio of (1:3), and then evaporated and diluted to a total volume of 10 mL. After filtration of the samples, Pt concentrations were determined by ICP-OES (Agilent Technologies) according to absorbance values and with correlation to calibration curves.

#### **CP-GNP dosing regimens in MB49 tumor-bearing mice**

For assessment of anti-tumor efficacy and safety of different dosing regimens, MB49 tumor-bearing mice received non-fractionated free CP or CP-GNP [single 20 mg/kg dose, IP; in accordance with single non-fractionated high cisplatin dose of ~70 mg/m<sup>2</sup> in cisplatin-eligible bladder cancer patients (Jiang et al. 2021)] and were then monitored over 2 weeks for tumor volume, weight, and survival. Another group of MB49

tumor-bearing mice received fractionated dosing of either free CP or CP-GNP (10 mg/kg on day 2, 7 mg/kg on day 6, and 3 mg/kg on day 12 and day 16; IP injection), and were monitored over 20 days for tumor volume, weight, and survival. Fractionated and non-fractionated regimens were based on established cisplatin-induced rodent models of kidney injury (Perše and Veceric-Haler 2018) and on clinical fractionated/non fractionated treatments for bladder cancer patients (Jiang et al. 2021). Untreated tumor-bearing mice served as control. Tumor growth measurements were conducted using a caliper and calculated according to standard formula ( $\text{length} \times \text{width}^2 \times 0.5$ ) (Sápi et al. 2015). Each group of mice was given its own code (without prior knowledge of the measurer) to ensure non-biased measurements.

### Histological analysis

For the non-fractionated protocol, mice ( $n=5-7$ ) were euthanized and taken for histology on day 4 after treatment. Prior to euthanasia, a weight decrease of over 30% (which indicates moribund condition) was validated in the free CP-treated mice. For the fractionated protocol, mice ( $n=5-7$  from each group) were euthanized at the conclusion of the study (day 20 after first treatment). Kidney was isolated and dissected in 4  $\mu\text{m}$ -thick sections. Sections were stained with hematoxylin and eosin (H&E) or Masson's trichrome stain and assessed under light microscope ( $\times 20$  magnification). Blinded (non-biased) pathological analysis and scoring [using a semi-quantitative 5-point grading scale of severity of histopathological changes (Schafer et al. 2018)] was conducted by Patho-Logica Ltd.

### Statistical analysis

Comparison of tumor growth rate and of data between two groups were performed using paired two-tailed Student's *t*-test. *p*-values below 0.05 were considered significant. Survival curves were calculated by Kaplan–Meier method. Chi-squared test ( $\chi^2$ ) was used for survival analysis.

### Supplementary Information

The online version contains supplementary material available at <https://doi.org/10.1186/s12645-023-00221-7>.

**Additional file 1: Figure S1.** Biodistribution of CP-GNPs. Accumulation of increasing doses of CP-GNP was measured in liver, spleen, kidney, lymph nodes and tumor of MB49-tumor bearing mice at 14 day post treatment using ICP-OES. Increasing doses of CP-GNP correlated with higher accumulation in liver, spleen and tumor. **Figure S2.** Biodistribution of free CP vs. CP-GNPs. A. Accumulation of free CP and CP-GNP was measured in liver, spleen, kidney, lymph nodes and tumor of MB49-tumor bearing mice 4 day post treatment using ICP-OES. Significantly higher doses of CP-GNP were measured in spleen, liver and tumor. B. Proportion analysis of Pt in different organs of free CP and CP-GNP treated mice. Results indicate that most of the CP is cleared in mice treated with free CP, while a significant amount of CP-GNP is still present in the different organs (0.02 vs. 0.15 mg Pt/gr tissue). Moreover, results indicate that in mice treated with free CP, the second most saturated organ with CP is the kidney as opposed to mice treated with CP-GNP in which the second most saturated organ is the spleen. **Figure S3.** Comparison of biodistribution of 20 mg/kg CP-GNPs at 4 days and 14 days after treatment. Accumulation of 20 mg/kg CP-GNP was measured using ICP-OES in liver, spleen, kidney, lymph nodes and tumor of MB49-tumor bearing mice at 4 and 14 day post-treatment.

### Acknowledgements

Not applicable.

### Author contributions

YS: conception, design, drafting; MM: acquisition analysis; CT-A: conception; TS: drafted and substantially revised the work, RP and ER: conception, design. All authors have approved the submitted version and have agreed both to be

personally accountable for the author's own contributions and to ensure that questions related to the accuracy or integrity of any part of the work, even ones in which the author was not personally involved, are appropriately investigated, resolved, and the resolution documented in the literature.

#### Funding

Not applicable.

#### Availability of data and materials

The data sets used and/or analysed during the current study are available from the corresponding author on reasonable request.

#### Declarations

##### Ethics approval and consent to participate

All experiments were conducted in mice and carried out under the Israeli Animal Protection Law and the regulations of the National Council for Animal Experimentation, in strict accordance with the guidelines for the European Community Council Directive (2010/63/EU) for Protection of Vertebrate Animals Used for Experimental and other Scientific Purposes; and in accordance with, and under strict supervision of, the Bar Ilan University Institutional Ethics Committee, as required by State and University regulations. The study complied with the ARRIVE guidelines (Animal Research: Reporting In Vivo Experiments). Bar Ilan University animal facility operates according to the Guide for the Care and Use of Laboratory Animals, DHEW (NIH, Pub. 78–23).

##### Consent for publication

Not applicable.

##### Competing interests

The authors declare no potential competing interest.

Received: 26 February 2023 Accepted: 16 July 2023

Published online: 01 September 2023

#### References

- Bourquin J, Milosevic A, Hauser D, Lehner R, Blank F, Petri-Fink A et al (2018) Biodistribution, clearance, and long-term fate of clinically relevant nanomaterials. *Adv Mater* 30(19):1704307
- Comenge J, Sotelo C, Romero F, Gallego O, Barnadas A, Parada TGC et al (2012) Detoxifying antitumoral drugs via nano-conjugation: the case of gold nanoparticles and cisplatin. *PLoS ONE* 7(10):e47562
- Dash A, Galsky MD, Vickers AJ, Serio AM, Koppie TM, Dalbagni G et al (2006) Impact of renal impairment on eligibility for adjuvant cisplatin-based chemotherapy in patients with urothelial carcinoma of the bladder. *Cancer* 107(3):506–513
- Davidi ES, Dreifuss T, Motiei M, Shai E, Bragilovski D, Lubimov L et al (2018) Cisplatin-conjugated gold nanoparticles as a theranostic agent for head and neck cancer. *Head Neck* 40(1):70–78
- Johnson SW, Stevenson JP, O'Dwyer PJ (2001). Cisplatin and Its Analogues. In: DeVita VT, Hellman S, Rosenberg SA (Eds), *Cancer: Principles and Practice of Oncology*, 6th edn., Lippincott Williams & Wilkins Publishers.
- Dreifuss T, Betzer O, Shilo M, Popovtzer A, Motiei M, Popovtzer R (2015) A challenge for theranostics: is the optimal particle for therapy also optimal for diagnostics? *Nanoscale* 7(37):15175–15184
- Duan X, He C, Kron SJ, Lin W (2016) Nanoparticle formulations of cisplatin for cancer therapy. *Wiley Interdiscip Rev Nanomed Nanobiotechnol* 8(5):776–791. <https://doi.org/10.1002/wnan.1390>
- Enustun BV, Turkevich J (1963) Coagulation of colloidal gold. *J Am Chem Soc* 85(21):3317–3328
- Gao Q, Zhang J, Gao J, Zhang Z, Zhu H, Wang D (2021) Gold nanoparticles in cancer theranostics. *Front Bioeng Biotechnol* 9(April):1–20
- Goldstein RS, Mayor GH (1983) The nephrotoxicity of cisplatin. *Life Sci* 32(7):685–690
- González-López MA, Gutiérrez-Cárdenas EM, Sánchez-Cruz C, Hernández-Paz JF, Pérez I, Olivares-Trejo JJ et al (2020) Reducing the effective dose of cisplatin using gold nanoparticles as carriers. *Cancer Nanotechnol* 11(1):1–15
- Hartmann JT, Kollmannsberger C, Kanz L, Bokemeyer C (1999) Platinum organ toxicity and possible prevention in patients with testicular cancer. *Int J Cancer* 83(6):866–869
- Hazkani I, Motiei M, Betzer O, Sadan T, Bragilovski D, Lubimov L et al (2017) Can molecular profiling enhance radiotherapy? Impact of personalized targeted gold nanoparticles on radiosensitivity and imaging of adenoid cystic carcinoma. *Theranostics* 7(16):3962–3971
- Hsu JC, Nieves LM, Betzer O, Sadan T, Noël PB, Popovtzer R et al (2020) Nanoparticle contrast agents for X-ray imaging applications. *Wires Nanomed Nanobiotechnol*. <https://doi.org/10.1002/wnan.1642>
- Huang Y, Wang J, Jiang K, Chung EJ (2021) Improving kidney targeting: the influence of nanoparticle physicochemical properties on kidney interactions. *J Control Release* 334(February):127–137
- Ichioka D, Miyazaki J, Inoue T, Kageyama S, Sugimoto M, Mitsuzuka K et al (2015) Impact of renal function of patients with advanced urothelial cancer on eligibility for first-line chemotherapy and treatment outcomes. *Jpn J Clin Oncol* 45(9):867–873
- Jiang DM, Gupta S, Kitchlu A, Meraz-Munoz A, North SA, Alimohamed NS et al (2021) Defining cisplatin eligibility in patients with muscle-invasive bladder cancer. *Nat Rev Urol* 18(2):104–114
- Kumar D, Saini N, Jain N, Sareen R, Pandit V (2013) Gold nanoparticles: an era in bionanotechnology. *Expert Opin Drug Deliv* 10(3):397–409

- Lavoie JM, Sridhar SS, Ong M, North S, Alimohamed N, McLeod D et al (2021) The rapidly evolving landscape of first-line targeted therapy in metastatic urothelial cancer: a systematic review. *Oncologist* 26(8):e1381–e1394
- Libutti SK, Paciotti GF, Byrnes AA, Alexander HR, Gannon WE, Walker M et al (2010) Phase I and pharmacokinetic studies of CYT-6091, a novel PEGylated Colloidal Gold-rhTNF nanomedicine. *Clin Cancer Res* 16(24):6139–6149
- Liu YR, Yin PN, Silvers CR, Lee YF (2019) Enhanced metastatic potential in the MB49 urothelial carcinoma model. *Sci Rep* 9(1):1–9
- Manohar S, Leung N (2018) Cisplatin nephrotoxicity: a review of the literature. *J Nephrol* 31(1):15–25
- Perazella MA (2012) Onco-nephrology: Renal toxicities of chemotherapeutic agents. *Clin J Am Soc Nephrol* 7(10):1713–1721
- Perazella MA, Moeckel GW (2010) Nephrotoxicity from chemotherapeutic agents: clinical manifestations, pathobiology, and prevention/therapy. *Semin Nephrol* 30(6):570–581
- Perše M, Vecerik-Haler Z (2018) Cisplatin-induced rodent model of kidney injury. *Biomed Res Int* 2018:1–29
- Popovtzer A, Mizrahi A, Motiei M, Bragilovski D, Lubimov L, Levi M et al (2016) Actively targeted gold nanoparticles as novel radiosensitizer agents: an in vivo head and neck cancer model. *Nanoscale* 8(5):2678–2685
- Pourmadadi M, Eshaghi MM, Rahmani E, Ajalli N, Bakhshi S, Mirkhaef H et al (2022) Cisplatin-loaded nanoformulations for cancer therapy: a comprehensive review. *J Drug Deliv Sci Technol* 1(77):103928
- Rastinehad AR, Anastos H, Wajswol E, Winoker JS, Sfakianos JP, Doppalapudi SK et al (2019) Gold nanoshell-localized photothermal ablation of prostate tumors in a clinical pilot device study. *Proc Natl Acad Sci U S A* 116(37):18590–18596
- Sápi J, Kovács L, Drexler DA, Kocsis P, Gajári D, Sápi Z (2015) Tumor volume estimation and quasi-continuous administration for most effective bevacizumab therapy. *PLoS ONE* 10(11):1–20
- Schafer KA, Eighmy J, Fikes JD, Halpern WG, Hukkanen RR, Long GG et al (2018) Use of severity grades to characterize histopathologic changes. *Toxicol Pathol* 46(3):256–265
- Shirali AC, Perazella MA (2014) Tubulointerstitial injury associated with chemotherapeutic agents. *Adv Chronic Kidney Dis* 21(1):56–63
- Sideris S, Aoun F, Zanaty M, Martinez NC, Latifyan S, Awada A et al (2016) Efficacy of weekly paclitaxel treatment as a single agent chemotherapy following first-line cisplatin treatment in urothelial bladder cancer. *Mol Clin Oncol* 4(6):1063–1067
- Stern JM, Kibanov Solomonov VV, Sazykina E, Schwartz JA, Gad SC, Goodrich GP (2016). Initial Evaluation of the Safety of Nanoshell-Directed Photothermal Therapy in the Treatment of Prostate Disease. *Int J Toxicol* 35(1):38–46.
- Stylianopoulos T (2013) EPR-effect: utilizing size-dependent nanoparticle delivery to solid tumors. *Ther Deliv* 4(4):421–423
- Wheate NJ, Walker S, Craig GE, Oun R (2010) The status of platinum anticancer drugs in the clinic and in clinical trials. *Dalton Trans* 39(35):8113–8127
- Zhang YN, Poon W, Tavares AJ, McGilvray ID, Chan WCW (2016) Nanoparticle–liver interactions: cellular uptake and hepatobiliary elimination. *J Control Release* 28(240):332–348

## Publisher's Note

Springer Nature remains neutral with regard to jurisdictional claims in published maps and institutional affiliations.

Ready to submit your research? Choose BMC and benefit from:

- fast, convenient online submission
- thorough peer review by experienced researchers in your field
- rapid publication on acceptance
- support for research data, including large and complex data types
- gold Open Access which fosters wider collaboration and increased citations
- maximum visibility for your research: over 100M website views per year

At BMC, research is always in progress.

Learn more [biomedcentral.com/submissions](https://biomedcentral.com/submissions)

